Available online at www.sciencedirect.com
SCIENCE DIRECT®
Chemical Physics Letters 420 (2006) 296–303
CHEMICAL PHYSICS LETTERS
www.elsevier.com/locate/cplett

Semiclassical IVR approach to rotational excitation of non-polar diatomic molecules by non-resonant laser pulses

Carlos A. Arango, William W. Kennerly, Gregory S. Ezra *

Department of Chemistry and Chemical Biology, Baker Laboratory, Cornell University, Ithaca, NY 14853-1301, United States

Received 26 October 2005
Available online 25 January 2006

Abstract

We apply the 'classic' semiclassical initial value representation (SC-IVR) approach to describe rotational excitation of non-polar diatomic molecules by intense short non-resonant laser pulses. We also investigate the applicability of the quantum mechanical sudden approximation. It is found that the SC-IVR approach gives accurate rotational excitation probabilities in regimes where the sudden approximation fails. Primitive semiclassical wavefunction propagation is used to illustrate the phenomenon of angular focussing of rotation states by strong pulses.

1. Introduction

There has been much recent interest, both theoretical and experimental, in rotational excitation and alignment of diatomic molecules using non-resonant laser pulses (for a review, see Ref. [1]). In the adiabatic regime, where the pulse is long on the timescale of molecular rotation, molecular alignment persists only for the duration of the pulse. In the opposite limit of very short pulses, coherent superpositions of rotor states are created that can exhibit post-pulse alignment [1,2].

Semiclassical methods are particularly appropriate for phenomena occurring on short timescales and are potentially applicable to systems with many degrees of freedom [3]. There has recently been a resurgence of interest in the development of semiclassical methods, especially SC-IVR (semiclassical initial value representation) approaches that avoid trajectory root searches (see below) [4,5]. The Herman–Kluk propagator based on harmonic oscillator coherent states has been widely used [5–7]. Although a few applications of the Herman–Kluk propagator have been made to problems involving rotational degrees of freedom (HCl dimer [8], constrained systems [9], particle on a ring [10]), there are fundamental difficulties inherent in the application of an approach based on cartesian coordinates and momenta to systems having essentially non-cartesian phase spaces [5,11].

In the present Letter, we apply traditional semiclassical methods [12] (i.e., not based on coherent states) to treat rotational excitation of non-polar diatomics by short non-resonant laser pulses. Given the well-known problems of primitive semiclassical *S*-matrix theory based on the Van Vleck–Gutzwiller propagator [13] due to the necessity for trajectory root searches and the occurence of amplitude divergences [12], we apply the 'classic' SC-IVR method [14,15] based on an IVR representation of the transition amplitude to compute rotational transition probabilities. (Schwieters and Delos have previously applied SC-IVR approaches to treat half-cycle pulse excitation of Rydberg atoms [16,17].) The SC-IVR approach is found to give excellent results for short pulses. Despite divergences at caustics, we apply the primitive SC approach to illustrate angular focussing of the ground state rotor wavefunction by short pulses [18]. The utility of the quantum sudden approximation for non-resonant laser pulses is also investigated, and compared with the SC-IVR approach.

In Section 2, we briefly review the classical and semiclassical theory of rotational excitation of non-polar diatomics

* Corresponding author. Fax: +1 607 255 4137.
E-mail address: gse1@cornell.edu (G.S. Ezra).

0009-2614/$ - see front matter © 2006 Elsevier B.V. All rights reserved.
doi:10.1016/j.cplett.2005.12.087

by non-resonant laser pulses. Particular attention is paid to the question of amplitude phases (Morse–Maslov indices [19]). In Section 3, we derive an approximate expression for rotational transition probabilities using the quantum mechanical sudden approximation (cf. [20,21]). Section 4 provides a comparison of exact (numerical) quantum transition probabilities and the SC-IVR results. It is seen that the SC-IVR results are valid in a regime where the quantum sudden approximation is not useful. In Section 5, we compute the time-dependent rotor wavefunction using primitive semiclassical theory, in order to illustrate angular focussing of the rotor by short pulses [18,22]. Section 6 concludes.

2. Semiclassical theory of rotational transitions in diatomics induced by non-resonant laser pulses

We consider rotational excitation of a non-polar diatomic molecule by an intense, high frequency, linearly polarized laser pulse. The laser frequency is assumed to be large (infrared) compared with the rotational frequency and not resonant with either molecular vibrational or electronic absorption frequencies, so that the molecule-laser interaction can be obtained by averaging the Hamiltonian over the laser cycle [1].

2.1. Classical Hamiltonian

In terms of free-rotor action-angle variables [3] the classical Hamiltonian for the 3D rotor is

$$H = \frac{j^2}{2I} - g(t)\Delta\omega\left(1 - \frac{m^2}{j^2}\right)\cos^2 q_j, \tag{1}$$

where j and m are the magnitude and the z-component, respectively, of the angular momentum vector $\boldsymbol{j}$, I is the moment of inertia, q_j is the angle variable conjugate to j [3], and $g(t)$ is the laser pulse envelope function. The quantity $\Delta\omega$ is proportional to the polarizability anisotropy: $\Delta\omega = (\varepsilon_L^2/4)(\alpha_\parallel - \alpha_\perp)$ [23], where ε_L is the peak laser field.

We shall take $g(t)$ to be a Gaussian centered at t_0 with full-width at half-maximum $\tau \approx (5/3)\sigma$ [2]

$$g(t) = \exp\left[-\frac{(t-t_0)^2}{\sigma^2}\right]. \tag{2}$$

Since the time-dependent perturbation does not depend on the angle q_m, m is a constant of the motion, and the magnitude of the molecule-field interaction is largest for $m = 0$. In this specific case the Hamiltonian is

$$H = \frac{j^2}{2I} - g(t)\Delta\omega\cos^2 q_j, \tag{3}$$

equivalent to a planar (2D) rotor. This time-dependent system can be studied in an extended phase space (j, q_j, t, p_t) with 'Hamiltonian'

$$K = \frac{j^2}{2I} - g(t)\Delta\omega\cos^2 q_j + p_t, \tag{4}$$

where the 'time' is now the auxiliary progress parameter s, and the associated canonical equations are:

$$\frac{dt}{ds} = \frac{\partial K}{\partial p_t} = 1, \tag{5a}$$

$$\frac{dp_t}{ds} = -\frac{\partial K}{\partial t} = -\frac{2\Delta\omega(t-t_0)}{\sigma^2}g(t)\cos^2 q_j, \tag{5b}$$

$$\frac{dq_j}{ds} = \frac{\partial K}{\partial j} = \frac{j}{I}, \tag{5c}$$

$$\frac{dj}{ds} = -\frac{\partial K}{\partial q_j} = -g(t)\Delta\omega\sin 2q_j. \tag{5d}$$

Since K is independent of s its value is conserved by the time evolution (5). Setting $K = 0$, Eq. (4) gives

$$p_t = -H = -\frac{j^2}{2I} + g(t)\Delta\omega\cos^2 q_j, \tag{6}$$

which yields the energy of the system at any time and provides the initial condition for p_t.

2.2. Classical interaction picture

The form of the Hamiltonian (1) allows the separation

$$H = H_0(j) + H_1(\varphi, t), \tag{7}$$

where H_0 is the free-rotor Hamiltonian, H_1 contains the interaction with the pulse, and we set $\varphi \equiv q_j$. In the classical interaction picture (CIP) the dynamical variables evolve forward in time according to the full Hamiltonian H then backward in time using the Hamiltonian H_0 [24]. The Hamiltonian in the CIP is obtained by a canonical transformation using an $F_3(j, \bar{\varphi}; t)$ generator [25], an explicit function of the old momentum j, the new angle $\bar{\varphi}$, and the time t

$$F_3(j, \bar{\varphi}; t) = -j\bar{\varphi} - Bj^2(t - t_0). \tag{8}$$

For this generating function we have [25]

$$\bar{j} = -\frac{\partial F_3}{\partial \bar{\varphi}} = j, \tag{9a}$$

$$\varphi = -\frac{\partial F_3}{\partial j} = \bar{\varphi} + 2Bj(t - t_0), \tag{9b}$$

$$\bar{H} = H + \frac{\partial F_3}{\partial t} = H - Bj^2 = -g(t)\Delta\omega\cos^2[\bar{\varphi} + 2Bj(t - t_0)]. \tag{9c}$$

For the CIP Hamiltonian (9c) the equations of motion are

$$\frac{d\bar{\varphi}}{dt} = \frac{\partial \bar{H}}{\partial j} = 2B(t - t_0)g(t)\Delta\omega\sin 2[\bar{\varphi} + 2Bj(t - t_0)], \tag{10a}$$

$$\frac{dj}{dt} = -\frac{\partial \bar{H}}{\partial \bar{\varphi}} = -g(t)\Delta\omega\sin 2[\bar{\varphi} + 2Bj(t - t_0)] \tag{10b}$$

with the additional equation

$$\frac{dp_t}{dt} = -\frac{\partial \bar{H}}{\partial t} = g'(t)\Delta\omega\cos^2[\bar{\varphi} + 2Bj(t - t_0)] - 2Bjg(t)\Delta\omega\sin 2[\bar{\varphi} + 2Bj(t - t_0)]. \tag{11}$$

The equation of motion for the stability matrix M [26] is

$$\frac{\mathrm{dM}}{\mathrm{d}t} = \mathsf{JHM}, \tag{12}$$

with J the fundamental symplectic matrix, and H the hessian matrix of the Hamiltonian.

2.3. Semiclassical quantized actions and energies

For simplicity, we shall consider the planar (2D) rotor only, both in classical and quantum mechanics, for which the Hamiltonian is identical to (3). For the 2D rigid rotor the semiclassically quantized actions are [3]

$$j = v\hbar, \quad v = 0, \pm 1, \pm 2, \ldots \tag{13}$$

with energy levels given by

$$E = \frac{j^2}{2I} = \frac{v^2\hbar^2}{2I}. \tag{14}$$

Precise knowledge of the angular momentum j implies complete uncertainty in the conjugate angle variable $q_j(\varphi)$ [3,12]. The semiclassical analogue of the 2D quantum state $|j\rangle$ is the circle $j = \text{const.}$, with angle φ uniformly distributed between 0 and 2π, $0 \leqslant \varphi \leqslant 2\pi$.

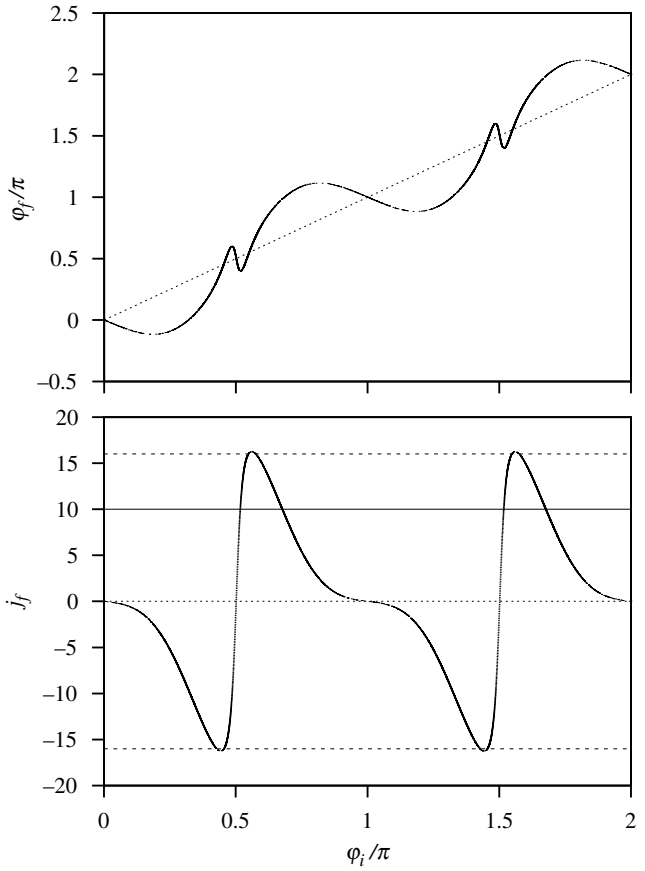

Fig. 1. Propagated final manifolds $\varphi_f(\varphi_i)$ and $j_f(\varphi_i)$. Initial manifolds are shown as dotted lines: $\varphi = \varphi_i$ (upper panel), and $j = 0$ (lower panel). In the lower panel the lines at $j = \pm 16$ are close to momentum space caustics.

The system described by Eq. (3) is essentially a free rotor for times $|t - t_0| \gg \sigma$. Rotational excitation is then studied classically by computing the time evolution of an ensemble of initial conditions associated with a given quantum state from a time well before ($t \to -\infty$) to a time well after ($t \to +\infty$) the arrival of the laser pulse. Final j values for individual trajectories in the ensemble will be constant and excitation/de-excitation probabilities can be determined.

To calculate rotational excitation probabilities using the primitive semiclassical S-matrix approach it is necessary to identify all root trajectories [12], those trajectories which start with quantizing actions j_i and end up with quantized final actions j_f as $t \to +\infty$. In Fig. 1, we show final manifolds $\varphi_f(\varphi_i)$ and $j_f(\varphi_i)$ corresponding to initial state $j_i = 0$. The initial manifolds are shown as dotted lines: the line $\varphi = \varphi_i$ for the upper panel, and $j = 0$ in the lower one. Note that, although in the second panel the root trajectories for $j = \pm 16$ are close to momentum space caustics, strictly necessitating a uniform SC treatment [27], there are no difficulties associated with fractal structure due to chaotic scattering ('chattering' [28,29]).

2.4. Semiclassical S-matrix expression for rotational transition amplitudes

Semiclassical transition amplitudes in the angular momentum representation are obtained from integral representations of the form [12]

$$\langle j_f|\mathrm{e}^{-\mathrm{i}\widehat{H}t/\hbar}|j_i\rangle = \int \mathrm{d}\varphi_f \langle j_f|\varphi_f\rangle\langle\varphi_f|\mathrm{e}^{-\mathrm{i}\widehat{H}t/\hbar}|j_i\rangle \tag{15}$$

with semiclassical wavefunction

$$\langle j_f|\varphi_f\rangle = (-2\pi\mathrm{i}\hbar)^{-\frac{1}{2}}\mathrm{e}^{-\mathrm{i}\varphi_f j_f/\hbar}. \tag{16}$$

Similarly the initial momentum to final coordinate amplitude is given in terms of the coordinate (angle) representation

$$\langle\varphi_f|\mathrm{e}^{-\mathrm{i}\widehat{H}t/\hbar}|j_i\rangle = \int \mathrm{d}\varphi_i \langle\varphi_f|\mathrm{e}^{-\mathrm{i}\widehat{H}t/\hbar}|\varphi_i\rangle\langle\varphi_i|j_i\rangle. \tag{17}$$

The Van Vleck–Gutzwiller semiclassical propagator in the coordinate representation is [13]

$$\langle\varphi_f|\mathrm{e}^{-\mathrm{i}\widehat{H}t/\hbar}|\varphi_i\rangle = (2\pi\mathrm{i}\hbar)^{-\frac{1}{2}}\sum_r \left|\frac{\partial^2 F_1(\varphi_f,\varphi_i;t)}{\partial\varphi_f\partial\varphi_i}\right|^{\frac{1}{2}} \times \exp\left[\frac{\mathrm{i}}{\hbar}F_1(\varphi_f,\varphi_i;t) - \mathrm{i}\frac{\pi}{2}\nu_r\right]. \tag{18}$$

with [25]

$$F_1(\varphi_f,\varphi_i;t) = \int_0^t \mathrm{d}t'[j_{t'}\dot{\varphi}_{t'} - H_{t'}] \tag{19}$$

and prefactor

$$\left|\frac{\partial^2 F_1(\varphi_f,\varphi_i;t)}{\partial\varphi_f\partial\varphi_i}\right|^{\frac{1}{2}} = \left|\frac{\partial\varphi_f}{\partial j_i}\right|^{-\frac{1}{2}}. \tag{20}$$

There will in general be several distinct root trajectories $z_t^{(r)}(z_i)$ going from $z_i = (\varphi_i, j_i)$ at time $t = 0$ to $z_f = (\varphi_f, j_f)$ at time t that contribute to the amplitude (18). (Note that, although the semiclassical expressions given in this section are implemented in the CIP, for notational convenience, we use φ rather than $\bar{\varphi}$ to denote the CIP angle.)

The primitive semiclassical amplitude (18) diverges at caustics (focal points), where $\frac{\partial \varphi_t}{\partial j_i} = 0$. In order for the primitive semiclassical amplitude (18) to be valid for times after the first or any succeeding caustic, it is necessary to include an extra time-dependent phase (Morse–Maslov index ν_r) [13,30]. This phase changes only when the trajectory crosses a caustic. (The time at which the kth caustic occurs, t_k^*, is called the kth focal time [19,31,13,32].) A general method for computing such phases was given by Maslov [30]. Campolieti and Brumer [19] have given explicit and computationally convenient formulas for general semiclassical amplitudes [19]. Although there are simpler ways of including the correct phase when a caustic is crossed [16,17], these are limited to systems with one degree of freedom. The formulas quoted in this section are the specialization to a single degree of freedom of the general formulas given in Ref. [19].

Inserting (18) into (15) and evaluating the integral by stationary phase, followed by substitution into (17) and a change of variable to φ_i we obtain the IVR integral representation of the transition amplitude in the momentum representation [14,19]

$$\langle j_f|e^{-i\widehat{H}t/\hbar}|j_i\rangle = (2\pi\hbar)^{-1}\int d\varphi_i \left|\frac{\partial \varphi_t}{\partial \varphi_i}\right|^{1/2} e^{-i\frac{\pi}{2}\nu(\varphi_i;t)} \times \exp\left\{\frac{i}{\hbar}[F_2(\varphi_f, j_i; t) - \varphi_t j_f]\right\}, \quad (21)$$

where [25]

$$F_2(\varphi_f, j_i; t) = F_1(\varphi_f, \varphi_i; t) + j_i\varphi_i. \quad (22)$$

and $\nu(\varphi_i; t)$ is the Maslov index for the initial condition φ_i at time $t_k^* < t < t_{k+1}^*$

$$\nu(\varphi_i; t) = \sum_k (1 - \sigma_k(\varphi_i))/2 \quad (23)$$

with

$$\sigma_k(\varphi_i) = \lim_{\epsilon\to 0} \operatorname{sgn}\left\{\frac{\partial \varphi_{t_k^*+\epsilon}(\varphi_i, j_i)}{\partial \varphi_i}\left[\frac{\partial \varphi_{t_k^*-\epsilon}(\varphi_i, j_i)}{\partial \varphi_i}\right]^{-1}\right\} \quad (24)$$

and sgn is the sign function. That is, the Maslov index changes after t_k^* only if $\sigma_k(\varphi_i) = -1$, i.e., if $\frac{\partial \varphi_t}{\partial \varphi_i}$ is negative (positive) before t_k^* and positive (negative) after t_k^*. Since this derivative cannot diverge this is equivalent to have a trajectory crossing a caustic $\frac{\partial \varphi_t}{\partial \varphi_i} = 0$ at t_k^*. Passage of the derivative $\frac{\partial \varphi_t}{\partial \varphi_i}$ through the value zero means that special attention must be given to the continuity of the integrand as a function of φ_i.

The computational advantage of formula (21) is that the prefactor never diverges. Moreover, it is not necessary to locate root trajectories, instead an integral over all possible values of $\varphi_{j,i}$ must be performed for each j_f. Possible problems arise from the fact that the integral (21) is oscillatory and the square root is not necessarily a smooth function of the initial angle. Note that the SC-IVR result is not a uniform SC approximation [5].

Evaluation of the integral (21) using the stationary phase approximation gives the primitive semiclassical (SC-SPA) expression [19]

$$\langle j_f|e^{-i\widehat{H}t/\hbar}|j_i\rangle = (2\pi i\hbar)^{-\frac{1}{2}}\sum_{\varphi_i^{(r)}} \left|\frac{\partial j_t}{\partial \varphi_i}\right|^{-\frac{1}{2}} \times \exp\left\{\frac{i}{\hbar}F_4(j_f, j_i; t) + i\frac{\pi}{2}\bar{\nu}(\varphi_i; t)\right\}, \quad (25)$$

where the sum involves all the root trajectories with $j = j_i$ at $t = 0$ and $j = j_f$ at the final time, the generating function [25]

$$F_4(j_f, j_i; t) = \int_0^t dt'\left[\varphi_{t'}\frac{dj_{t'}}{dt'} - H_{t'}\right], \quad (26)$$

and the Maslov index for the ith root trajectory in $t_k^* < t < t_{k+1}^*$ is [19]

$$\bar{\nu}(\varphi_i; t) = -\frac{1}{2}\left[1 + \operatorname{sgn}\frac{\partial j(0^+)}{\partial \varphi_i}\right] + \sum_k \Delta\bar{\nu}_k(\varphi_i). \quad (27)$$

As the elapsed time passes through the value t_k, the index changes by an amount

$$\Delta\bar{\nu}_k(\varphi_i) = \lim_{\epsilon\to 0}\frac{1}{2}(\sigma_k - 1)\operatorname{sgn}\frac{\partial j_\epsilon(\varphi^*, j^*)}{\partial \varphi^*}, \quad (28)$$

with $\varphi^* = \varphi_{t_k^*-\epsilon}(\varphi_i, j_i), j^* = j_{t_k^*-\epsilon}(\varphi_i, j_i)$, and

$$\sigma_k(\varphi_i) = \operatorname{sgn}\left\{\frac{\partial j_{t_k^*-\epsilon}(\varphi_i, j_i)}{\partial \varphi_i}\left[\frac{\partial j_{t_k^*+\epsilon}(\varphi_i, j_i)}{\partial \varphi_i}\right]^{-1}\right\}. \quad (29)$$

Again the Maslov index changes only if $\sigma_k(\varphi_i) = -1$, but now this change could be positive or negative depending on the sign of the partial derivative in (28).

The total primitive semiclassical amplitude (25) is obtained by adding the amplitudes of the root trajectories. The probability of a transition from j_i to j_f is given by

$$P_{j_i\to j_f} = \hbar^2|\langle j_f|j_i\rangle|^2. \quad (30)$$

Use of Eq. (25) requires knowledge of all the root trajectories. For a given j_i and $j_f = J_f$ these trajectories are obtained from the curve $j_f(\varphi_i)$ as shown in Fig. 1, where we have $j_i = 0$ and $\sigma = 0.04$. It can be seen that $\varphi_i = 0, \pi/2, \pi, 3\pi/2$ are fixed points of Eq. (10). Root trajectories for $j_f = \pm 16$ are close to the momentum space caustics, while the line $j_f = 0$ has an inflection point at $\varphi_i \approx 0, \pi$. For the case $j_f = 10$, for example, there are four root trajectories with initial angles $\varphi_i^{(r)}$, $r \in \{1, 2, 3, 4\}$. For each of the initial conditions it is necessary to obtain, at the final time, the stability matrix component $\partial j_t/\partial \varphi_i$, the accumulated value of the line integral F_4 (defined in Eq. (26)), and also the accumulated Maslov index $\bar{\nu}(\varphi_i; t)$, obtained via Eqs.

27,27,29, and thereby calculate the associated complex amplitude. In practice we interpolate the curves of final $\partial j_t/\partial\varphi_i$, F_4, and $\bar{v}(\varphi_i;t)$ at the root values of φ_i instead of doing the calculation over for the root trajectories alone. The calculation of the SC-IVR transition probabilities proceeds similarly; in this case the integral (21) over initial angles must be done.

A comparison of semiclassical and quantum results (exact and within the sudden approximation) is given in Section 4.

3. Quantum mechanical sudden approximation

For very short pulses ($\sigma \ll 1/B$) the use of the quantum sudden approximation is appropriate [33]. The propagator for Hamiltonian (1) over the time interval $t=0$ to $t=T$, where $0 \leqslant t_0 \leqslant T$ and the pulse intensity is practically zero at 0 and T, is approximated as [20]

$$\widehat{U}(T,0) \simeq e^{i\beta\cos^2\varphi} e^{-iT\widehat{H}_0/\hbar}, \tag{31}$$

where $\widehat{H}_0$ is the Hamiltonian for the free 2D-rotor and β is obtained as

$$\hbar\beta = -\int_0^T g(t')\Delta\omega\,dt' = -\sqrt{\pi}\sigma\Delta\omega, \tag{32}$$

for the Gaussian pulse described by (2), where we set the integration limits to $\pm\infty$ in evaluating the integral. For initial state $\psi_0(\varphi) = (2\pi)^{-1/2} e^{ij_0\varphi}$, the post-pulse state is

$$\psi_t(\varphi) = \widehat{U}(T,0)\psi_0(\varphi) = e^{i\beta\cos^2\varphi} e^{-iTE_{j_0}/\hbar}\psi_0(\varphi). \tag{33}$$

Expanding in terms of rotor eigenfunctions $\psi_j(\varphi) = (2\pi)^{-1/2} e^{ij\varphi}$, we have

$$\psi_t(\varphi) = \sum_{j\in\mathbb{Z}} c_M(T)\psi_j(\varphi) e^{-iTE_j/\hbar} \tag{34}$$

with coefficients

$$c_j(T) = \frac{1}{2\pi} e^{iT(E_j-E_{j_0})/\hbar} \int_0^{2\pi} e^{i\beta\cos^2\varphi} e^{-i\varphi\Delta j}\,d\varphi \tag{35a}$$

$$= \frac{1}{2} e^{iT(E_j-E_{j_0})/\hbar} e^{i\beta/2} i^{\Delta j/2} J_{\frac{\Delta j}{2}}(\beta/2)(1+e^{-i\pi\Delta j}) \tag{35b}$$

where $\Delta j = j - j_0$ and $J_\nu(z)$ is the usual Bessel function. Associated probabilities for transitions $j_0 \to j$ are

$$P_{j_0\to j} = |c_j(T)|^2 = \frac{1+\cos(\pi\Delta j)}{2}\left[J_{\frac{\Delta j}{2}}(\beta/2)\right]^2. \tag{36}$$

Thus, within the sudden approximation $P_{j_0\to j} = 0$ if Δj is odd. For Δj even, we have

$$P_{j_0\to j} = \left[J_{\frac{\Delta j}{2}}(\beta/2)\right]^2, \quad \Delta j \text{ even}. \tag{37}$$

The effectiveness of the sudden approximation for short pulses is shown in Fig. 2. For a pulse of width $\sigma = 0.02$ (upper panel) there is almost perfect agreement for all the transition probabilities for small $\Delta\omega$. For larger values of $\Delta\omega$ the results of the approximation are slightly different from the numerically determined (exact) quantum transition probabilities [34]. For a longer pulse of width $\sigma = 0.04$ (lower panel) the sudden approximation works well for $\Delta\omega < 200$ but yields worse results for larger values of $\Delta\omega$.

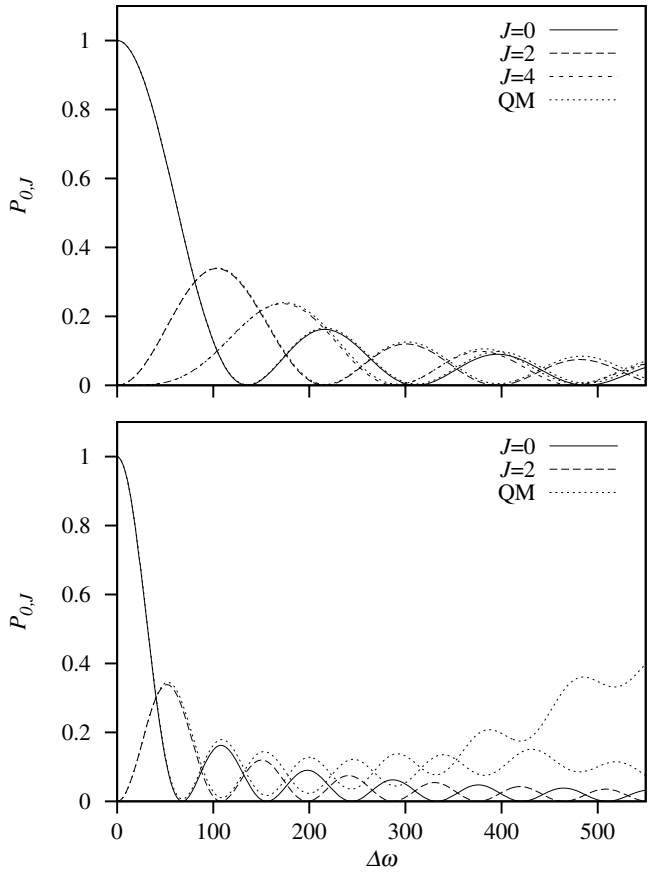

Fig. 2. Comparison of quantum sudden approximation and exact numerical quantum transition probabilities for short pulses. Initial state $J=0$. (Upper panel) $\sigma = 0.02$. Sudden approximation and exact quantum values are in good agreement for transition probabilities $J=0\to 0$, $0\to 2$ and $0\to 4$ for the range of laser intensities shown, $0 \leqslant \Delta\omega \leqslant 500$. (Lower panel) $\sigma = 0.04$. For the longer pulses, the sudden approximation begins to fail for $\Delta\omega > 200$.

4. Comparison of semiclassical and quantum results

To compare with dimensionless quantum results the classical rotational constant is set to the value $B=1$. For the short pulses studied here we have $\sigma \ll 1/B\hbar$. Another relevant parameter in the calculations is the dimensionless interaction strength $\Delta\omega$, for which the physical range of values is between 0 and 800 [23]. 5000 trajectories were used to evaluate the SC-IVR integral, 2000 trajectories for the SPA calculation.

Fig. 3 shows primitive and SC-IVR transition probabilities for a 2D rotor starting in the ground state $j=0$ for the case of an intense ($\Delta\omega = 400$) short pulse ($\sigma = 0.04\hbar/B$). Both semiclassical methods obey the symmetry selection rule $\Delta j = \pm 2$ for the 2D rotor in a linearly polarized laser field [12]. In contrast to the IVR results, the primitive SC

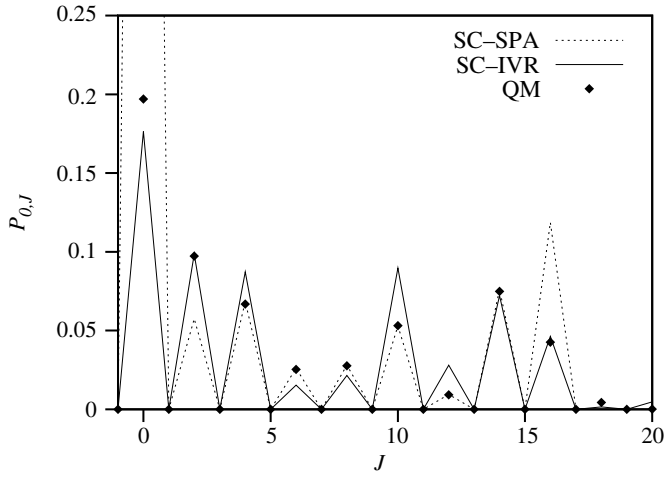

Fig. 3. Primitive (SC-SPA, -------), SC-IVR semiclassical (—) and quantum (♦) rotational transition probabilities from the ground state $J = 0$ for a 2D rotor in an intense, short laser pulse ($\Delta\omega = 400$, $\sigma = 0.04\hbar/B$). The primitive transition probabilities at $J = 0, \pm 16$ fail due to the proximity to momentum caustics. Only probabilities for $J \geqslant 0$ are shown; for initial state $J = 0$, we have $P_{0\to -J} = P_{0\to J}$.

approximation fails completely for the transition probabilities $P_{0\to 16}$ and $P_{0\to 0}$ due to the proximity of momentum caustics.

For the parameters of Fig. 3, the primitive semiclassical results are in better agreement with the exact quantum results than the SC-IVR for several final J values. Fig. 4 provides a more global picture for pulses of width $\sigma = 0.04$ and 0.08, and clearly shows the overall superiority of the SC-IVR method. The longer pulses ($\sigma = 0.08$) lead to more complicated caustic structure of the final manifolds, so that the primitive SC method essentially fails completely.

5. Semiclassical angular focussing of 2D-rotors

As the laser pulse reaches its maximum intensity at $t = t_0$ the rotor is subject to a strong periodic double-well potential in the angle φ with maxima at $\varphi = \pi/2, 3\pi/2$ and minima at $\varphi = 0, \pi$. For an initial quantized state with small quantum number j, the pulse causes a localization or focusing of trajectories near the minima of the potential energy [18]. This focusing, among other phenomena, has been studied recently for 2D and 3D kicked rotors [18,22].

The primitive semiclassical approximation for the initial momentum to final coordinate amplitude [12] including the Maslov index and considering all root trajectories is

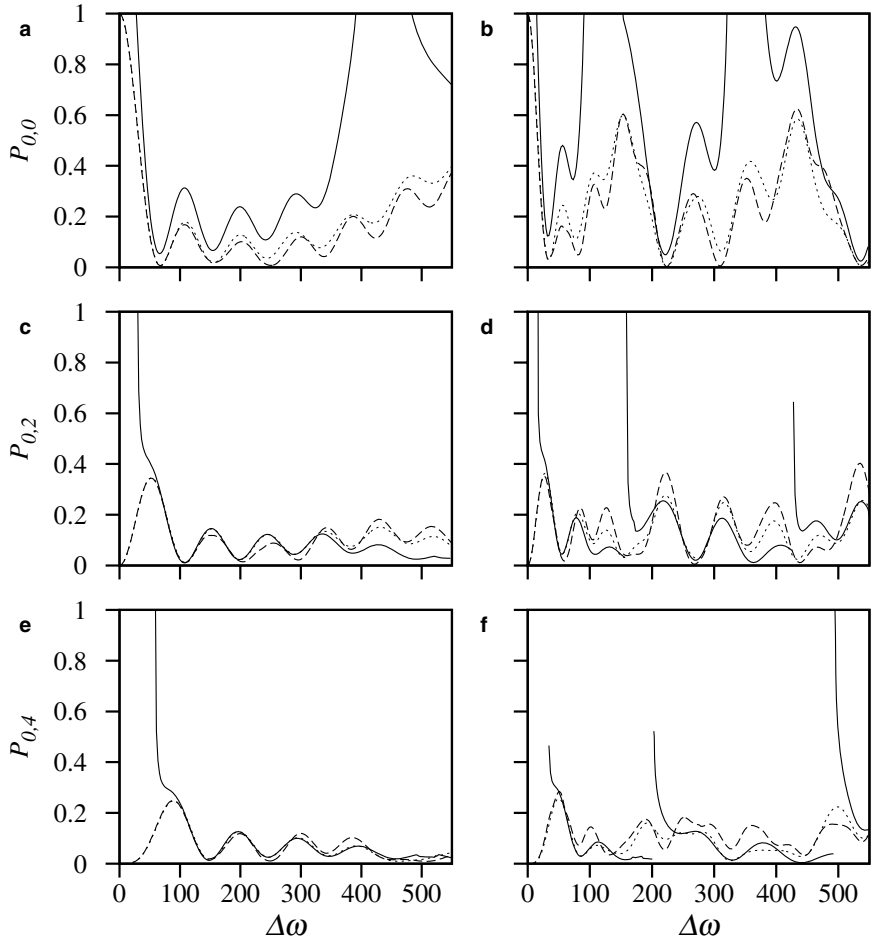

Fig. 4. Primitive semiclassical (solid line), SC-IVR (dashed line) and quantum (short dashed line) $P_{0\to J}$ rotational transition probabilities versus pulse intensity $\Delta\omega$: (a) $J = 0$, $\sigma = 0.04$; (b) $J = 0$, $\sigma = 0.08$; (c) $J = 2$, $\sigma = 0.04$; (d) $J = 2$, $\sigma = 0.08$; (e) $J = 4$, $\sigma = 0.04$; (f) $J = 4$, $\sigma = 0.08$.

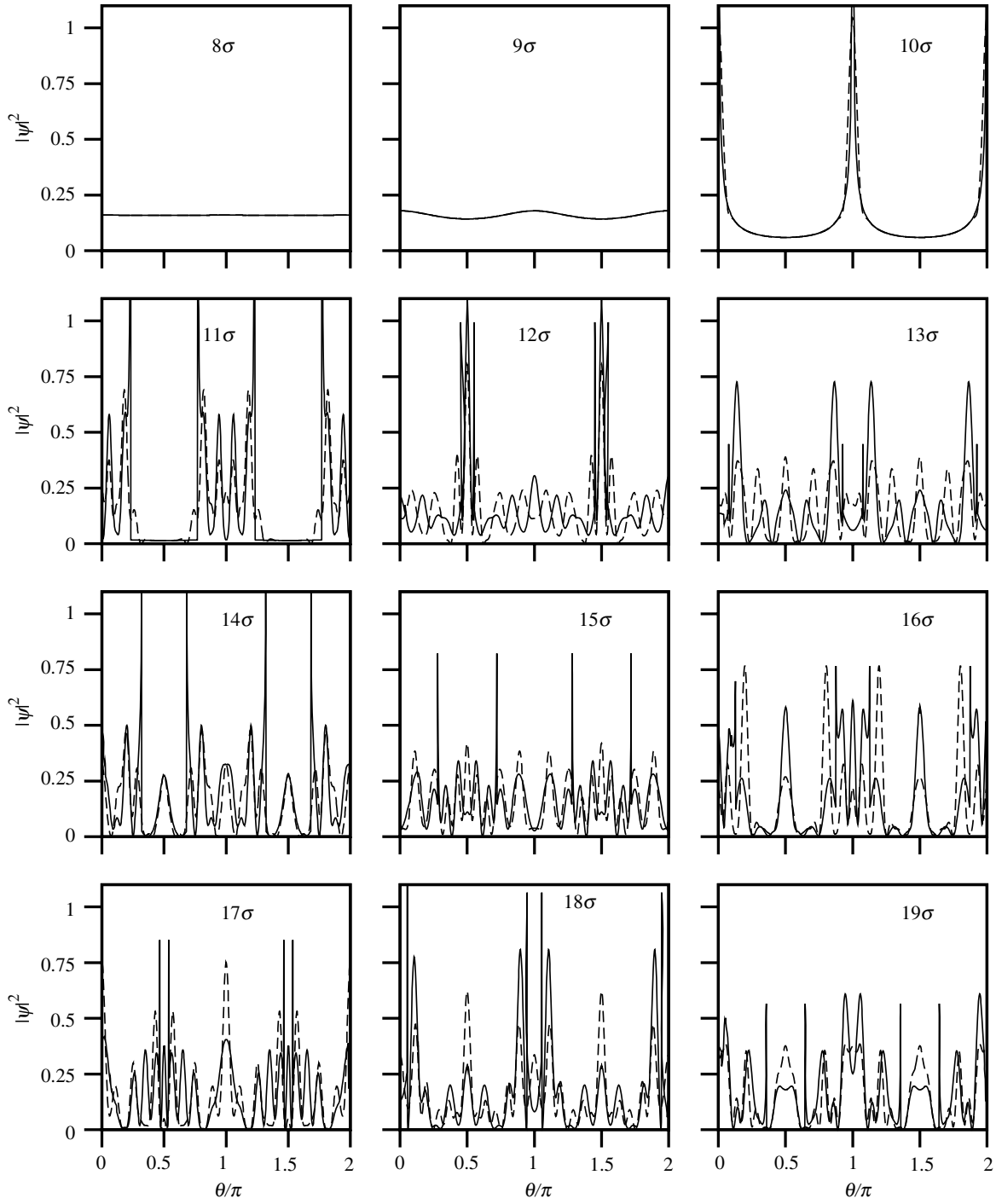

Fig. 5. Primitive semiclassical (—) and quantum (-------) probability densities for a 2D rotor initially in the ground state $J = 0$ subject to a pulse with $\Delta\omega = 400$, $\sigma = 0.04\hbar/B$. The legend for each panel indicates the elapsed time in units of the pulse width σ. The center of the pulse is at 10σ.

$$\langle\varphi_{\mathrm{f}}|\mathrm{e}^{-\mathrm{i}\widehat{H}t/\hbar}|j_{\mathrm{i}}\rangle = (2\pi\mathrm{i}\hbar)^{-\frac{1}{2}}\sum_{r}\left|\frac{\partial\varphi_t}{\partial\varphi_{\mathrm{i}}}\right|^{-\frac{1}{2}} \times \exp\left[\frac{\mathrm{i}}{\hbar}F_2(\varphi_{\mathrm{f}}, j_{\mathrm{i}}; t) - \mathrm{i}\frac{\pi}{2}\nu(\varphi_{\mathrm{i}}; t)\right] \qquad (38)$$

with $\nu(\varphi_{\mathrm{i}}, t)$ given by Eq. (23).

The semiclassical initial state is the line of initial conditions with constant j_{i} and $0 \leqslant \varphi_{\mathrm{i}} \leqslant 2\pi$. This initial manifold is propagated classically until time $t = t_{\mathrm{f}}$, when the curve $\varphi_{\mathrm{f}}(\varphi_{\mathrm{i}})$ is used to obtain root trajectories corresponding to a particular final angle φ_{f}. Using Eq. (38) we obtain a semiclassical wave function at $t = t_{\mathrm{f}}$ corresponding to the initial state $j_{\mathrm{i}} = J_{\mathrm{i}}\hbar = 0$. Fig. 5 shows associated probability densities $P(\varphi) = |\langle\varphi|\mathrm{e}^{-\mathrm{i}\widehat{H}t/\hbar}|j_{\mathrm{i}}\rangle|_2$ for a Gaussian pulse with $\Delta\omega = 400$, $\sigma = 0.04\hbar/B$, centered at $t_0 = 10\ \sigma$. The primitive semiclassical propagation yields acceptable agreement

with the quantum results [34], and shows qualitatively the focussing effect [18].

6. Conclusions

In this Letter, we have demonstrated the efficacy of standard semiclassical methods [12] for analyzing rotational excitation of non-polar diatomic molecules (planar rotors) by short non-resonant laser pulses. We have also investigated the applicability of the quantum mechanical sudden approximation. Comparison with converged numerical quantum results shows the sudden approximation to be accurate for very short pulses ($\sigma = 0.02$) but less accurate for only slightly longer pulses ($\sigma = 0.04$). Despite well-known failings of primitive semiclassical transition probabilities, the semiclassical IVR approach yields very accurate results, even in a regime where the sudden approximation fails. Finally, we have shown that primitive semiclassical wavefunctions provide a qualitatively correct description of angular focussing of rotational states by short laser pulses [18].

References

[1] H. Stapelfeldt, T. Seideman, Rev. Mod. Phys. 75 (2003) 543.
[2] J. Ortigoso, M. Rodriguez, M. Gupta, B. Friedrich, J. Chem. Phys. 110 (1999) 3870.
[3] M.S. Child, Semiclassical Mechanics with Molecular Applications, Oxford University Press, New York, 1991.
[4] W.H. Miller, J. Phys. Chem. A 105 (2001) 2942.
[5] K.G. Kay, Ann. Rev. Phys. Chem. 56 (2005) 255.
[6] M.F. Herman, E. Kluk, Chem. Phys. 91 (1984) 27.
[7] M.F. Herman, Annu. Rev. Phys. Chem. 45 (1994) 83.
[8] X. Sun, W.H. Miller, J. Chem. Phys. 108 (1998) 8870.
[9] B.B. Harland, P.N. Roy, J. Chem. Phys. 118 (2003) 4791.
[10] B. Balzer, S. Dilthey, G. Stock, M. Thoss, J. Chem. Phys. 119 (2003) 5795.
[11] K.G. Kay, J. Phys. Chem. A 105 (2001) 2535.
[12] W.H. Miller, Adv. Chem. Phys. XXV (1974) 69.
[13] M.C. Gutzwiller, Chaos in Classical and Quantum Mechanics, Springer, New York, 1990.
[14] W.H. Miller, J. Chem. Phys. 53 (1970) 3578.
[15] R.A. Marcus, J. Chem. Phys. 54 (1971) 3965.
[16] C.D. Schwieters, J.B. Delos, Phys. Rev. A 51 (1995) 1023.
[17] C.D. Schwieters, J.B. Delos, Phys. Rev. A 51 (1995) 1030.
[18] I.S. Averbukh, R. Arvieu, Phys. Rev. Lett. 87 (2001) (Art. No. 163601).
[19] G. Campolieti, P. Brumer, Phys. Rev. A 50 (1994) 997.
[20] M. Persico, P. VanLeuven, Z. fur Phys. D 41 (1997) 139.
[21] G. Granucci, M. Persico, P. VanLeuven, J. Chem. Phys. 120 (2004) 7438.
[22] M. Leibscher, I.S. Averbukh, P. Rozmej, R. Arvieu, Phys. Rev. A 69 (2004) (Art. No. 032102).
[23] B. Friedrich, D. Herschbach, J. Phys. Chem. A 103 (1999) 10280.
[24] R.T. Skodje, Chem. Phys. Lett. 109 (1984) 221.
[25] H. Goldstein, C. Poole, J. Safko, Classical Mechanics, third edn., Addison-Wesley, San Francisco, 2002.
[26] A.J. Lichtenberg, M.A. Lieberman, Regular and Chaotic Dynamics, second edn., Springer, New York, 1992.
[27] H. Kreek, R.L. Ellis, R.A. Marcus, J. Chem. Phys. 62 (1975) 913.
[28] C.C. Rankin, W.H. Miller, J. Chem. Phys. 55 (1971) 3150.
[29] L. Gottdiener, Mol. Phys. 29 (1975) 1585.
[30] V.P. Maslov, M.V. Fedoryuk, Semiclassical Approximations in Quantum Mechanics, Reidel, Boston, 1981.
[31] J.B. Delos, Adv. Chem. Phys. 65 (1986) 161.
[32] R.G. Littlejohn, J. Stat. Phys. 68 (1992) 7.
[33] L.I. Schiff, Quantum Mechanics, McGraw-Hill, New York, 1968.
[34] W.W. Kennerly, Ph.D. Thesis, Cornell University, 2005.